The Plant Journal (2007) **50**, 886–901 doi: 10.1111/j.1365-313X.2007.03099.x

The transcription factor HIG1/MYB51 regulates indolic glucosinolate biosynthesis in *Arabidopsis thaliana*

Tamara Gigolashvili[1], Bettina Berger[1], Hans-Peter Mock[2], Caroline Müller[3], Bernd Weisshaar[4] and Ulf-Ingo Flügge[1,*]
[1]*Botanisches Institut der Universität zu Köln, Gyrhofstrasse 15, D-50931 Köln, Germany,*
[2]*Institut für Pflanzengenetik und Kulturpflanzenforschung, Corrensstrasse 3, D-06466 Gatersleben, Germany,*
[3]*Julius-von-Sachs-Institut für Biowissenschaften, Universität Würzburg, Julius-von-Sachs-Platz 3, D-97082 Würzburg, Germany, and*
[4]*Lehrstuhl für Genomforschung, Universität Bielefeld, D-33594 Bielefeld, Germany*

Received 11 December 2006; revised 6 February 2007; accepted 15 February 2007.
*For correspondence (fax + 49 221 4705039; e-mail ui.fluegge@uni-koeln.de).

Summary

Glucosinolates are a class of plant secondary metabolites that serve as antiherbivore compounds in plant defence. A previously identified *Arabidopsis thaliana* activation-tagged line, displaying altered levels of secondary metabolites, was shown here to be affected in the content of indolic and aliphatic glucosinolates. The observed chemotype was caused by activation of the R2R3-MYB transcription factor gene *HIG1* (*HIGH INDOLIC GLUCOSINOLATE 1*, also referred to as *MYB51*). HIG1/MYB51 was shown to activate promoters of indolic glucosinolate biosynthetic genes leading to increased accumulation of indolic glucosinolates. The corresponding loss-of-function mutant *hig1-1* contained low levels of glucosinolates. Overexpression of the related transcription factor *ATR1/MYB34*, which had previously been described as a regulator of indolic glucosinolate and indole-3-acetic acid homeostasis, in the *hig1-1* mutant background led to a partial rescue of the mutant chemotype along with a severe high-auxin growth phenotype. Overexpression of *MYB122*, another close homologue of *HIG1*/*MYB51*, did not rescue the *hig1-1* chemotype, but caused a high-auxin phenotype and increased levels of indolic glucosinolates in the wild-type. By contrast, overexpression of *HIG1*/*MYB51* resulted in the specific accumulation of indolic glucosinolates without affecting auxin metabolism and plant morphology. Mechanical stimuli such as touch or wounding transiently induced the expression of *HIG1*/*MYB51* but not of *ATR1*/*MYB34*, and *HIG1/MYB51* overexpression reduced insect herbivory as revealed by dual-choice assays with the generalist lepidopteran herbivore, *Spodoptera exigua*. We hypothesize that HIG1/MYB51 is a regulator of indolic glucosinolate biosynthesis that also controls responses to biotic challenges.

Kewords: MYB factor, secondary metabolites, auxin, plant defence, biotic stress

Introduction

Glucosinolates are a class of nitrogen- and sulphur-containing plant secondary metabolites, which are mainly found in members of the Brassicaceae family including the model plant *Arabidopsis thaliana* (Rask *et al.*, 2000; Kliebenstein *et al.*, 2001; Mithen, 2001). Their role in plant defence against microorganisms (Mari *et al.*, 1996; Manici *et al.*, 2000) and herbivores (Kliebenstein *et al.*, 2002a; Levy *et al.*, 2005; Mewis *et al.*, 2005), as well as their importance in the human diet as inducers of anticarcinogenic enzymes (Shapiro *et al.*, 1998; Gross *et al.*, 2000; Mithen *et al.*, 2003; Grubb and Abel, 2006), attracted increased attention to this particular group of plant secondary metabolites.

Depending on the nature of the amino acid side chain, glucosinolates can be grouped into aliphatic, aromatic and indolic glucosinolates. The biosynthesis of glucosinolates comprises (i) chain elongation of the amino acids, (ii) formation of the glucosinolates by cytochrome P450 monooxygenases (CYPs), C-S lyases, *S*-glucosyltransferases and sulfotransferases, and (iii) secondary modifications (reviewed by Grubb and Abel, 2006).

The composition of glucosinolates can drastically vary in different ecotypes of *A. thaliana* (Kliebenstein *et al.*, 2001; Reichelt *et al.*, 2002), during ontogenesis (Petersen *et al.*, 2002; Brown *et al.*, 2003) or in response to environmental

stimuli (Brader *et al.*, 2001; Kliebenstein *et al.*, 2002b; Mikkelsen *et al.*, 2003; Bednarek *et al.*, 2005; Mewis *et al.*, 2005). Indolic glucosinolates are mainly found in vegetative parts of plants, rosette leaves and roots, whereas highest concentrations of aliphatic glucosinolates are found in seeds, flowers and siliques (Brown *et al.*, 2003). Recent studies have shown that genes encoding enzymes of the indolic glucosinolate biosynthetic pathway form stable co-expression clusters, and group together with tryptophan biosynthetic genes in response to stress conditions (Gachon *et al.*, 2005).

Synthesis of indolic glucosinolates in *A. thaliana* starts with the formation of indole-3-acetaldoxime (IAOx) from tryptophan, a step catalysed by CYP79B2/CYP79B3. IAOx can subsequently serve as a substrate for CYP83B1 resulting in the formation of 1-*aci*-nitro-2-indolyl-ethane, but is simultaneously a precursor for indole-3-acetic acid (IAA, auxin) biosynthesis. An interplay between the IAA and indolic glucosinolate biosynthetic pathways could be demonstrated by the analysis of several loss-of-function and gain-of-function mutants. For example, *A. thaliana* plants overexpressing CYP79B2 showed an increased accumulation of both indolic glucosinolates and IAA; conversely, the *cyp79B2/cyp79B3* double mutant is impaired in the synthesis of indolic glucosinolates, but only partially in IAA biosynthesis, suggesting the existence of other IAA precursors besides IAOx (Zhao *et al.*, 2002). Mutants defective in *CYP83B1* (*SUR2*) show a high-IAA phenotype accompanied by reduced levels of indolic glucosinolates (Barlier *et al.*, 2000; Bak and Feyereisen, 2001; Smolen and Bender, 2002). A total lack of indolic glucosinolates was not observed, presumably because *CYP83A1*, involved in the synthesis of aliphatic glucosinolates, can partially compensate for the defect in *CYP83B1* (Naur *et al.*, 2003). Interestingly, the *cyp83B1* phenotype correlates with that of the *ugt74B1* mutant, which is defective in the next and penultimate step of indolic glucosinolate biosynthesis: the formation of desulfoglucosinolate (Grubb *et al.*, 2004).

Although the functional role of several indolic glucosinolate biosynthetic pathway genes has been studied for quite some time, the first regulatory components for this pathway were identified only recently. A calmodulin-binding nuclear protein, IQD1, was shown to be a positive regulator of aliphatic and indolic glucosinolate formation (Levy *et al.*, 2005). Overexpression of *IQD1* resulted in increased levels of both indolic and aliphatic glucosinolates, thereby enhancing plant defence against generalist herbivores, whereas the levels of both types of glucosinolates were decreased in *iqd* loss-of-function mutants. Likewise, the R2R3-MYB transcription factor ATR1/MYB34, along with its known role in tryptophan biosynthesis (Bender and Fink, 1998), appears to control homeostasis between indolic glucosinolate and IAA biosyntheses (Celenza *et al.*, 2005). Furthermore, a DNA-binding-with-one-finger (AtDof1.1) transcription factor has recently been shown to be part of the regulatory network controlling glucosinolate biosynthesis (Skirycz *et al.*, 2006). Here, we present functional evidence that HIG1/MYB51 represents a transcriptional regulator of indolic glucosinolate biosynthesis genes in *A. thaliana*. Expression of *HIG1/MYB51* responds to mechanical stimuli like touch or wounding, and overexpression of HIG1/MYB51 results in increased plant resistance against generalist herbivores.

Results

Identification of the HIG1/MYB51 gene and properties of the HIG1 protein

The *HIGH PHENOLIC COMPOUND1-1 DOMINANT* (*HPC1-1D*) mutant was isolated in a previously described screen of the *A. thaliana* activation-tagged TAMARA population for mutant plants containing increased levels of phenolic compounds (Schneider *et al.*, 2005). Although the *HPC1-1D* activation-tagged mutant did not show any informative growth phenotype, HPLC profiling of *HPC1-1D* revealed an increased accumulation of an unknown metabolite in the mutant by between four- and sixfold when compared with wild-type plants (Schneider *et al.*, 2005). Using preparative and analytical HPLC analysis in combination with mass spectrometry, this compound was subsequently identified as desulfo-indolic glucosinolate or desulfo-glucobrassicin (indol-3-ylmethyl glucosinolate, see Figure S1). The *HPC1-1D* mutant was therefore renamed as *HIG1-1D* (*HIGH INDOLIC GLUCOSINOLATE1-1 DOMINANT*).

The insertion position of the *dSpm-Act* element in the *HIG1-1D* mutant has been localized to chromosome 1, approximately 1.4 kb upstream of At1g18570. Several genes encoding proteins of unknown or hypothetical functions are located adjacent to the insertion site of the non-autonomous recombinant transposon carrying the 4x35S enhancer. Analysis of mRNA levels by RT-PCR demonstrated an obvious overexpression of At1g18570 in the activation-tagged *HIG1-1D* mutant relative to the wild-type, whereas expression of the other adjacent gene At1g18560 encoding a transposase-related protein was neither detected in wild-type plants nor in the mutant line (Schneider *et al.*, 2005). Steady-state mRNA expression levels of other neighbouring genes – At1g18590 (the desulfoglucosinolate sulfotransferase AtST5c; Piotrowski *et al.*, 2004), At1g18580 (a glucosyltransferase family protein) and At1g18550 (a kinesin motor related protein) – were not affected in *HIG1-1D* mutant plants (not shown), corroborating our previous finding that the observed metabolic phenotype of the mutant is caused by ectopic overexpression of At1g18570.

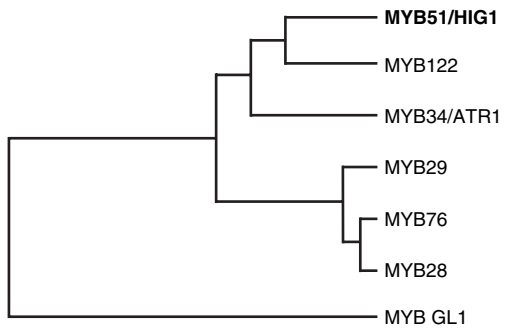

Figure 1. *HIG1/MYB51* belongs to the subgroup 12 of the *Arabidopsis thaliana* R2R3-MYB gene family.
Amino acid sequences from the six members of R2R3-MYB factors assigned to subgroup 12 that share the common amino acid motif [L/F]LN[K/R]VA (Stracke *et al.*, 2001) and the amino acid sequence of GL1 (Glabrous1) were downloaded from Genbank. The distance tree was constructed by aligning the sequences with CLUSTAW and DIALIGN-T, and by using PHYLIP with the BLOSUM62 matrix. The bootstrap support for all nodes is better than 87, except for the separation of MYB76 and MYB28.

The results summarized above demonstrate that At1g18570 is the gene responsible for the *HIG1-1D* phenotype. The gene product of At1g18570 is MYB51, a member of subgroup 12 of the large family of R2R3-MYB transcription factors (Figure 1). We refer to this gene as *HIGH INDOLIC GLUCOSINOLATE 1* (*HIG1/MYB51*). The *HIG1/MYB51* gene structure exhibiting three exons and two introns was confirmed by isolation and sequencing of the full-length cDNA. The predicted protein is 352 amino acid residues in length with a molecular mass of about 39 kDa and a calculated isoelectric point of 5.6. The sequence displays similarities in PFAM and PROSITE motifs (PS00037, PS50090, PS00334 and PF00249.18) to known nuclear localized proteins (as found at http://www.expasy.org). HIG1/MYB51 does not contain a typical nuclear localization signal (NLS) as revealed by PredictNLS (http://cubic.bioc.columbia.edu/services/predictNLS/; Nair and Rost, 2005); however, an amino acid residue stretch KKRLIKK was detected (amino acid residues 114–120) that might act as a SV40-type NLS. Similar motifs are also present in sequences of other members of the HIG1/MYB51 subfamily (KKRLKQK and KKCLVKK in the case of ATR1/MYB34 and MYB122, respectively), suggesting that these motifs could actually direct the proteins to the nucleus.

To determine the subcellular localization of the HIG1/MYB51 transcription factor in plant cells, a translational fusion of the full-length *HIG1/MYB51* coding sequence with the open reading frame encoding the GFP was generated. The localization of the fusion protein was analyzed in transfected BY2 tobacco protoplasts, as well as in cultured *A. thaliana* (Col-0) cells and in transiently transformed *A. thaliana* leaves. In all systems, a nuclear localization of the HIG1:GFP fusion protein could be demonstrated (Figure S2).

The glucosinolate contents of HIG1-1D *plants,* HIG1/MYB51 *overexpression lines and the* hig1-1 *loss-of-function mutant*

We constructed lines that overexpress *HIG1/MYB51* under control of the *CaMV 35S* promoter in the wild-type background, and isolated a *hig1* null mutant (GABI-Kat line 228B12, Col-0 background, harbouring a T-DNA insertion in the second exon of *HIG1/MYB51*; the mutant and the allele is referred to as *hig1-1*).

To analyze whether the glucosinolate levels are affected by changes in *HIG1/MYB51* expression, the glucosinolate accumulation pattern of *HIG1-1D* was analyzed along with that of *HIG1/MYB51* overexpression lines and that of the homozygous *hig1-1* mutant, which does not express *HIG1/MYB51* (see Figure 2a). Three out of ten representative overexpressing lines [*35S:HIG1-3(wt), -7(wt)* and *-8(wt)*] are shown in more detail together with *HIG1-1D* and *hig1-1* (Figure 2b and c). As expected, indol-3-ylmethyl glucosinolate (I3M) was accumulated to sixfold higher levels in the *HIG1-1D* mutant (Figure 2b) than in the wild-type. Likewise, the overexpression lines contained increased levels of I3M by between three- and eightfold compared with the wild-type. There was also an increase in the other main indolic glucosinolate 4MOI3M (and 1MOI3M) level in both *HIG1-1D* and the overexpression lines compared with the wild-type.

Notably, the activation of indolic glucosinolate biosynthesis in both *HIG1-1D* and the overexpression lines was accompanied by the downregulation of the main aliphatic glucosinolate 4MSOB (Figure 2b). However, the total quantity of glucosinolates (aliphatic plus indolic) was increased in *HIG1-1D* and the overexpression lines up to threefold (Figure 2c), with *HIG1/MYB51* transcript levels being correlated with the indolic glucosinolate levels in the respective lines (Figure 2a). Hence, the chemotype of *35S:HIG1* overexpression lines reproduced that of *HIG1-1D*. All overexpressing lines possessed an unchanged growth phenotype, as is the case for *HIG1-1D* and the *hig1-1* mutant (see below).

As also shown in Figure 2, the accumulation of tryptophan- and methionine-derived glucosinolates was decreased in *hig1-1* (see 4MSOB and I3 M in Figure 2b), and the total glucosinolate content was reduced to almost one third compared with the wild-type. Plants that overexpress *HIG1/MYB51* in the background of *hig1-1* are indistinguishable from *HIG1/MYB51* overexpression lines in the Col-0 background with respect to all analysed chemotypic and growth phenotype parameters (Figure S3).

HIG1/MYB51 trans-*activates the expression of indolic glucosinolate biosynthetic pathway genes*

We analyzed the ability of *HIG1/MYB51* to activate promoters of genes involved in the indolic glucosinolate biosynthetic pathway (Figure 3) using co-transformation assays. *A. thaliana* leaves were infiltrated with (i) a supervirulent

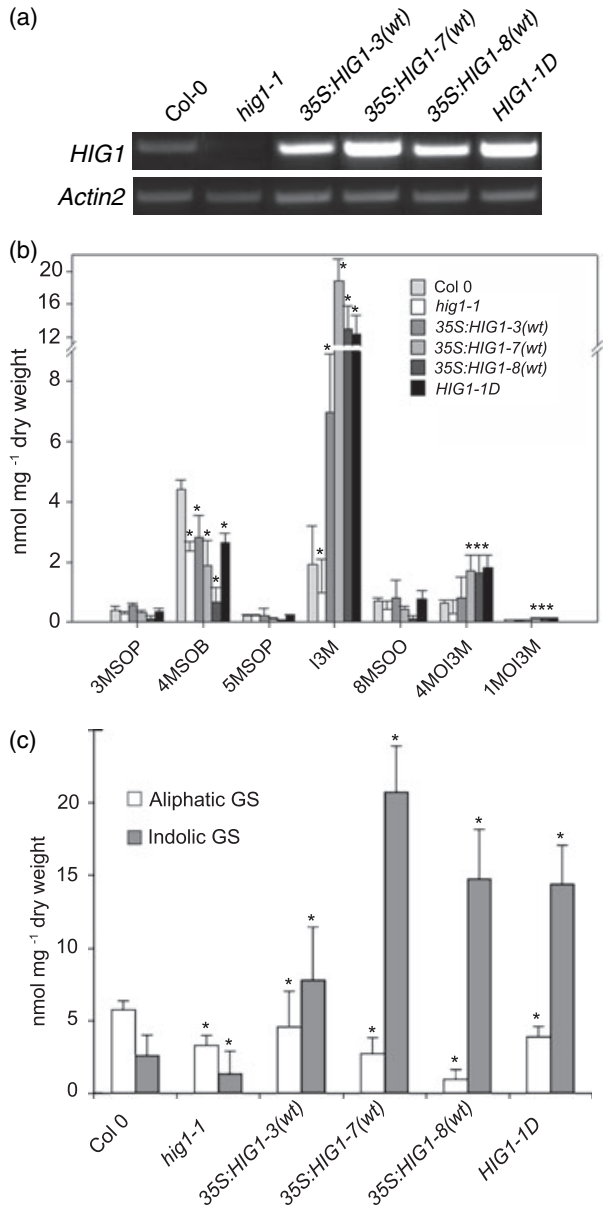

Figure 2. Glucosinolate (GS) contents and steady state levels of *HIG1*/*MYB51* mRNA transcripts in rosette leaves of 5-week-old wild-type plants, loss-of-function mutant *hig1-1, 35S:HIG1* overexpressing lines and the activation-tagged line *HIG1-1D*.

(a) Semi-quantitative analysis of steady-state mRNA level of *HIG1*/*MYB51* in wild-type (wt) (Col-0), *hig1-1,* three independent overexpression lines [*35S:HIG1-3(wt), 35S:HIG1-7(wt)* and *35S:HIG1-8(wt)*], and *HIG1-1D*. Total RNA was prepared from rosette leaves of 5-week-old plants, and gene-specific primers for *HIG1*/*MYB51* and *Actin2* genes were used. Each PCR assay (22–26 cycles) was repeated three times with two independent sets of plants.

(b) Glucosinolate contents in the different lines (means ± SD, $n = 3$). GS was extracted from freeze-dried rosette leaves of 5-week-old plants. 3MSOP, 3-methylsulfinylpropyl-GS; 4MSOB, 4-methylsulfinylbutyl-GS; 5MSOP, 5-methylsulfinylpentyl-GS; 4MTB, 4-methylthiobutyl-GS; I3M, indol-3-yl-methyl-GS; 8MSOO, 8-methylsulfinyloctyl-GS; 4MOI3M, 4-methoxyindol-3-ylmethyl-GS; 1MOI3M, 1-methoxyindol-3-ylmethyl-GS.

(c) Content of bulk of glucosinolates in wild-type, *hig1-1*, overexpressing lines *35S:HIG1-3(wt)*, *35S:HIG1-7(wt)* and *35S:HIG1-8(wt)*, and *HIG1-1D*.

*Significantly different (Student's *t* test; $P < 0.05$) in comparison with wild-type.

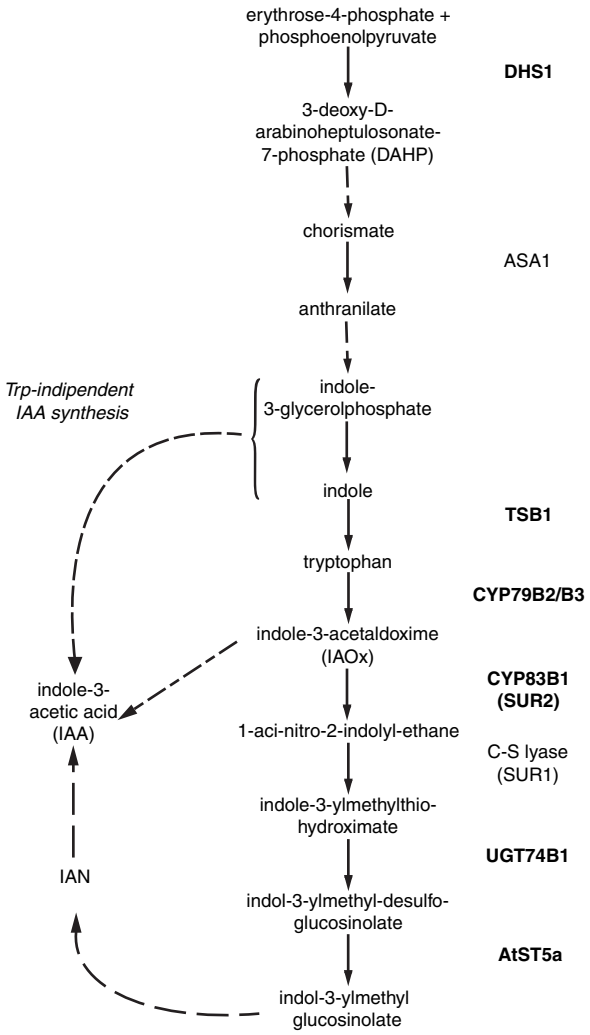

Figure 3. Proposed pathways for indolic glucosinolate and indole-3-acetic acid (IAA) biosyntheses.

Targets genes of *HIG1*/*MYB51* are shown in bold. Proposed IAA synthesis from the indolic glucosinolate indol-3-ylmethyl glucosinolate is indicated by a dotted arrow (Pollmann *et al.*, 2002). IAN, indole-3-acetonitrile.

Agrobacteria strain LBA4404.pBBR1MCS.virGN54D (kindly provided by Dr Memelink, University of Leiden) carrying the *35S:HIG1* construct for effector expression and/or (ii) one of several different reporter constructs containing the *uidA* (GUS) gene driven by the promoter of putative target genes (*DHS1, ASA1, TSB1, CYP79B2, CYP79B3, CYP83B1 and AtST5a*). Leaves transiently expressing only the GUS reporter constructs fused to promoters of target genes showed only weak GUS activity, whereas co-transformation with *35S:HIG1* led to a significant increase in GUS expression demonstrating the potential of *HIG1/MYB51* to *trans*-activate the respective promoters (Figure 4). All tested promoters except for *ASA1* were activated by *HIG1*/*MYB51* indicating that *HIG1*/*MYB51* positively regulates indolic glucosinolate biosynthetic pathway genes.

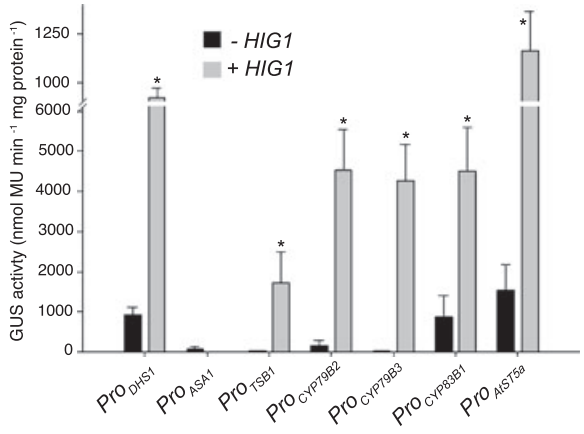

Figure 4. *HIG1/MYB51* activates glucosinolate biosynthetic pathway genes. Co-transformation assays to determine the target-gene specificity for *HIG1/MYB51* (effector) towards target promoters of indolic biosynthetic pathway genes (means of GUS activity in nmol methylumbelliferone (MU) per min and mg protein ± SD, $n = 5$). The promoters of *DHS1*, *ASA1*, *TSB1*, *CYP79B2*, *CYP79B3*, *CYP83B1 and AtST5a* genes were fused to the *uidA* (GUS) reporter gene (*TargetPromoter:GUS* vectors). Fully expanded leaves of *Arabidopsis thaliana* plants were infiltrated with the supervirulent Agrobacterium strain LBA4404.pBBR1MCS.virGN54D containing either the reporter construct (*TargetPromoter:GUS:pGWB3i*) and a 'null' effector (empty vector without *HIG1/MYB51*, *35S*:pGWB2) or the target gene fused to the reporter (*TargetPromoter:GUS:pGWB3i*) and, in addition, the *HIG1/MYB51* effector (*35S:HIG1:pGWB2*). Black bars represent expression of only the *TargetPromoter:GUS* constructs with 'null' effector, grey bars represent the expression of *TargetPromoter:GUS* constructs co-transformed with *35S:HIG1*.
*Significantly different (Student's *t* test; $P < 0.05$) in comparison with the 'null vector' control.

Overexpression of ATR1/MYB34 *and* MYB122 *in wild-type and the* hig1-1 *mutant: analysis of growth phenotypes and auxin contents*

As evident from Figure 1, *HIG1/MYB51* is a member of a group of related *R2R3-MYB* genes (subgroup 12), with *MYB122* as the closest and *ATR1/MYB34* as the next homologue. MYB122 has to our knowledge not yet been functionally analyzed, whereas ATR1/MYB34 has been implicated in the regulation of indolic glucosinolate biosynthesis. Therefore, we studied the effect of ectopic overexpression of *ATR1/MYB34* and *MYB122*, respectively, in both *hig1-1* mutant (m) and wild-type (wt) genetic backgrounds. Both coding sequences were driven by the *CaMV 35S* promoter.

Interestingly, all lines overexpressing *ATR1/MYB34* in the *hig1-1* mutant background [from 70 primary transformants, nine lines were analyzed in detail, two of which, *35S:ATR1-22(m)* and *35S:ATR1-24(m)*, are presented in Figure 5a] showed highly retarded shoot and root growth, curly leaves, a bushy stature and were unable to produce seeds. This phenotype is clearly indicative of high IAA levels in the plants.

Ectopic overexpression of *ATR1/MYB34* in wild-type background [from 70 primary transformants, eight lines were analyzed in detail, three of which, *35S:ATR1-17(wt), 35S:ATR1-1(wt) and 35S:ATR1(wt)* (not further analyzed), are presented in Figure 5a] led to a similar high-IAA phenotype. Generally, the expression level of the transgene in both genetic backgrounds correlated with the strength of the high-IAA phenotype. Anyway, most of the flowers of *35S:ATR1* overexpressing plants stayed closed until senescence or developed tiny mal-developed siliques (Figure 5a, inset).

In contrast to plants overexpressing *ATR1/MYB34* in *hig1-1* or wild-type background, overexpression of *MYB122* in the *hig1-1* mutant background [from 70 primary transformants, eight lines were analyzed in detail, two of which, *35S:MYB122-8(m) and 35S:MYB122-11(m)*, are presented in Figure 5a] did not result in an aberrant growth phenotype. However, in the wild-type background (Col-0), several MYB122 overexpressing lines {from 70 primary transformants, seven lines were analyzed in detail, two representative lines with either a moderate [*35S:MYB122-6(wt)*] or a strong [*35S:MYB122-16(wt)*] phenotype are shown in Figure 5a} displayed a high-IAA phenotype, even though this was less pronounced than in the case for *ATR1/MYB34* overexpressing lines. *35S:MYB122-16(wt)* plants were retarded in growth: most of the flowers stayed undeveloped and were almost unable to produce healthy siliques, albeit some seeds could be collected for further propagation.

We also measured the levels of free IAA in these different lines (Figure 5b). Although the IAA levels in the activation-tagged *HIG1-1D* mutant and in *hig1-1* did not significantly differ from that in the wild-type, the ATR1/MYB34 overexpression lines possessed threefold [*35S:ATR1-17(wt),* moderate phenotype in the wild-type background] and up to sevenfold higher IAA levels in plants with a more severe growth phenotype [*35S:ATR1-1(wt), 35S:ATR1-22(m)* and *35S:ATR1-24(m)*]. Interestingly, auxin levels of MYB122 overexpression lines in the *hig1-1* background remained unchanged, but increased by between two- and fivefold when *MYB122* was overexpressed in the wild-type background. Thus, the levels of free IAA nicely corresponded to the observed growth phenotypes: none of the *HIG1/MYB51* overexpressing lines showed an aberrant growth phenotype neither in the wild-type nor in the *hig1-1* background (Figure 5a; Figure S3). By contrast, all *ATR1/MYB34* overexpression lines and strong *MYB122* overexpression lines in the wild-type background showed a high-IAA phenotype.

It has been previously suggested that nitrilases could be involved in the production of additional IAA under particular physiological conditions (Bartel and Fink, 1994; Grsic-Rausch *et al.*, 2000; Pollmann *et al.*, 2006). Nitrilases convert indole-3-acetonitrile (IAN), produced from the indolic glucosinolate I3M, into IAA (Figure 3). The observation that the expression of the *NITRILASE 2* gene is dramatically increased in *ATR1/MYB34* overexpression lines, but not in *HIG1/MYB51* and *MYB122* overexpression lines, might shed new light on the high-IAA chemotype of *ATR1/MYB34* overexpressing lines (Figure S4).

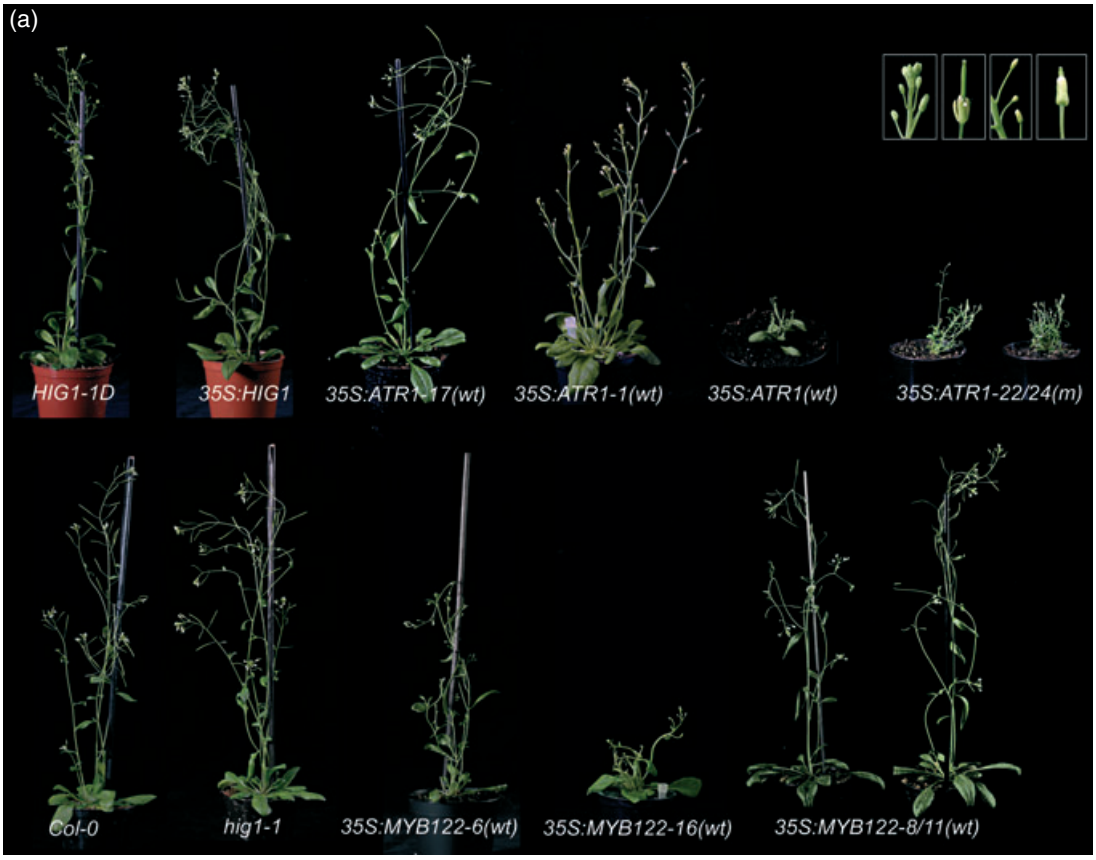

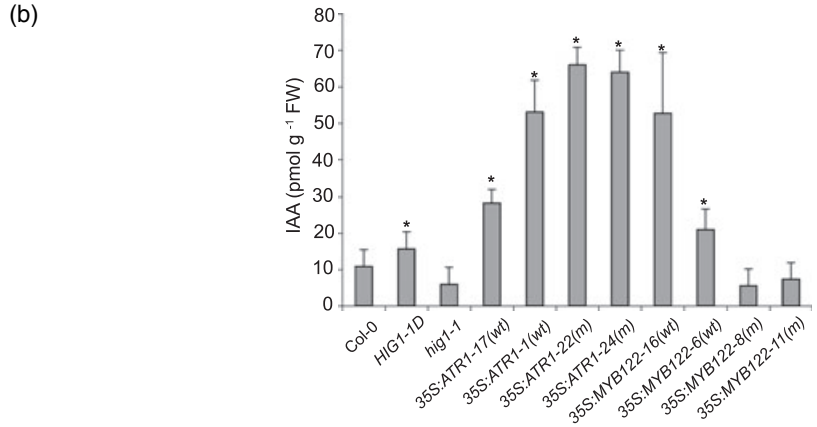

Figure 5. Growth phenotypes of wild-type plants and *hig1-1* mutants expressing *ATR1*/*MYB34* or *MYB122* constructs, and determination of corresponding auxin levels.
(a) Different independent transgenic lines are shown: the abbreviation given in brackets indicates the genetic background, i.e either wild-type (wt) or the *hig1-1* background (m). Upper row, from the left to the right: *HIG1-1D, 35S:HIG1, 35S:ATR1-17(wt), 35S:ATR1-1(wt)* [lines harbouring the construct in the Col-0 background exhibiting a high indole-3-acetic acid (IAA) phenotype], *35S:ATR1(wt)* (line harbouring the *35S:ATR1* construct in the Col-0 background exhibiting a strong growth phenotype), *35S:ATR1-22(m)* and *35S:ATR1-24(m)* (lines harbouring the *35S:ATR1* construct in the *hig1-1* background exhibiting a high-IAA phenotype). Lower row from the left to the right: wild-type (Col-0), *hig1-1*, *35S:MYB122-6(wt)* and *35S:MYB122-16(wt)* (lines harbouring the *35S:MYB122* construct in the Col-0 background exhibiting a high-IAA phenotype and a strong growth phenotype), *35S:MYB122-8(m)* and *35S:MYB122-11(m)* (lines harbouring the *35S:MYB122* construct in the *hig1-1* background [no IAA phenotype]). Inset: defective flowers and siliques peculiar for *35S:ATR1* overexpressing plants, independent of the genetic background, and for *35S:MYB122* in the wild-type background.
(b) Free indole-3-acetic acid (IAA) concentrations in leaves of wild-type, *HIG1-1D*, *hig1-1*, *ATR1*/*MYB34* and *MYB122* overexpression plants. *35S:ATR1-17(wt) and 35S:ATR1-1(wt), ATR1/MYB34* overexpressed in the wild-type background; *35S:ATR1-22(m) and 35S:ATR1-24(m), ATR1/MYB34* overexpressed in the *hig1-1* background; *35S:MYB122-16(wt) and 35S:MYB122-6(wt), MYB122* overexpressed in the wild-type background; *35S:MYB122-8(m)* and *35S:MYB122-11(m), MYB122* overexpressed in the *hig1-1* background. Data are mean values ± SD of three individual experiments ($n = 3$). *Significantly different (Student's *t* test; $P < 0.05$) in comparison with the wild-type. For details, see Experimental procedures.

Overexpression of ATR1/MYB34 and MYB122 in wild-type and the hig1-1 mutant: analysis of chemotypes and indolic glucosinolate pathway genes

We also analyzed if the *hig1-1* mutant chemotype characterized by lower contents of glucosinolates could be rescued by overexpression of *ATR1*/*MYB34* or *MYB122*. Results are shown in Figure 6a for the two *ATR1*/*MYB34* overexpressing lines in the *hig1-1* background [*35S:ATR1-22(m)* and *35S:ATR1-24(m)*] and, for comparison, in the wild-type background [*35S:ATR1-1(wt)* and *35S:ATR1-17(wt)*], respectively. All lines except for *35S:ATR1-17(wt)* showed higher contents of both the main indolic and aliphatic glucosinolates I3M and 4MSOB compared with the *hig1-1* mutant. The levels of I3M are also up to 1.7-fold higher compared with the wild-type, but clearly lower compared with the overexpressing line *HIG1-1D* (which shows a sixfold increase in the I3M level). The level of 4MOI3M, which is enhanced in *HIG1-1D*, was not affected in *ATR1/MYB34* overexpression lines. It should be noted that the level of aliphatic glucosinolates (e.g. 4MSOB) are lower in *HIG1-1D* compared with the wild-type (see Figure 2).

Figure 6b shows that the low indolic glucosinolate chemotype of the *hig1-1* mutant could not be converted towards the wild-type phenotype by overexpression of *MYB122* [lines *35S:MYB122-8(m)* and *35S:MYB122-11(m)*]. However, strong overexpression of *MYB122* in the wild-type background [line *35S:MYB122-16(wt)*] led to a significant increase in I3M levels.

We also addressed the question of whether or not the recorded metabolite and IAA profiles are supported by expression profiling data of indolic glucosinolate and IAA biosynthetic genes. As shown in Figure 6c and d, transcript levels of *ASA1*, *TSB1*, *CYP79B2*, *CYP79B3* and *CYP83B1* were upregulated in all *ATR1*/*MYB34* overexpression lines, independent of the genetic background, and in *MYB122* overexpression lines in the wild-type background [*35S:MYB122-16(wt)*]. In the *hig1-1* background [lines *35S:MYB122-8(m)* and *35S:MYB122-11(m)*], *MYB122*, although expressed to high levels, was obviously not able to upregulate any of the target genes that could be activated in the wild-type background. Notably, expression levels of indolic glucosinolate biosynthetic pathway genes further downstream of *CYP83B1*, i.e. *UGT74B1* and *AtST5a*, were not significantly affected, neither by *ATR1/MYB34* nor by *MYB122* overexpression.

Taken together, all genes of indolic glucosinolate biosynthesis (from TSB1 to the last enzyme AtST5a) are activated by *HIG1*/*MYB51* (Figures 4 and 6c,d). *ATR1*/*MYB34* and *MYB122* can also positively regulate glucosinolate biosynthesis genes, but overexpression of *ATR1/MYB34*, independently of the genetic background, led to a high-IAA phenotype, as is the case for overexpression of *MYB122* in the wild-type background. This might be caused by the accumulation of IAOx, which could be shuttled into alternative metabolic pathways such as the biosynthesis of IAA.

Tissue-specific expression of HIG1/MYB51

To study the tissue-specific expression of *HIG1*/*MYB51*, the promoter region (from –1676 to + 342 bp), including the first intron and the first exon of the *HIG1*/*MYB51* coding sequence, was used to generate a translational fusion with the *uidA* (GUS) reporter gene. This construct was stably transferred to *A. thaliana* plants by *Agrobacterium tumefaciens*-mediated transformation. Of the 15 transgenic Pro_{HIG1}*:uidA* lines that were analyzed in detail, 12 lines showed a similar tissue-specific pattern of *HIG1*/*MYB51* expression. Histochemical analysis of GUS activity revealed a strong reporter gene expression already in the hypocotyl of 3-day-old seedlings (Figure 7). Although the cotyledons showed no GUS activity at this stage, they were clearly stained at a later stage of ontogenesis. Furthermore, GUS activity was detected in the roots of young seedlings. In newly emerging rosette leaves, GUS staining was only faint and primarily visible around the midvein and at the base of trichomes. Reporter gene activity increased gradually in expanding leaves, reaching a maximum in fully expanded leaves, where the mesophyll tissue also showed GUS staining. During senescence, GUS expression disappeared almost completely, but was still detectable in the vasculature. Furthermore, expression was present in primary and lateral roots of plants at the rosette stage. In the floral tissue, GUS activity was only detected in young flowers but not at later stages of development. Siliques showed very faint staining in an early stage, and GUS activity was restricted to the abscission zone in fully developed siliques.

Overall, *HIG1*/*MYB51* promoter activity was strongest in the vegetative parts of the plants, mainly in mature rosette leaves. *HIG1*/*MYB51* expression can also be observed in roots, but not in mature flowers or siliques. By contrast, analysis of Pro_{ATR1}*:uidA* plants revealed that *ATR1*/*MYB34* is mainly expressed in meristematic tissues and young flowers, but not in leaves, which are the main site of indolic glucosinolate biosynthesis and accumulation (Figure S5). Notably, the tissue-specific expression data for both *HIG1*/*MYB51* and *ATR1*/*MYB34* are consistent with AtGenExpress data from the Genevestigator microarray database (Zimmermann *et al.*, 2004; http://www.genevestigator.ethz.ch/).

HIG1/MYB51 *expression is induced by mechanical stimuli like touch and wounding*

Glucosinolates play a major role in plant defence against herbivore attack, normally accompanied by wounding. Because HIG1/MYB51 is potentially involved in the control of

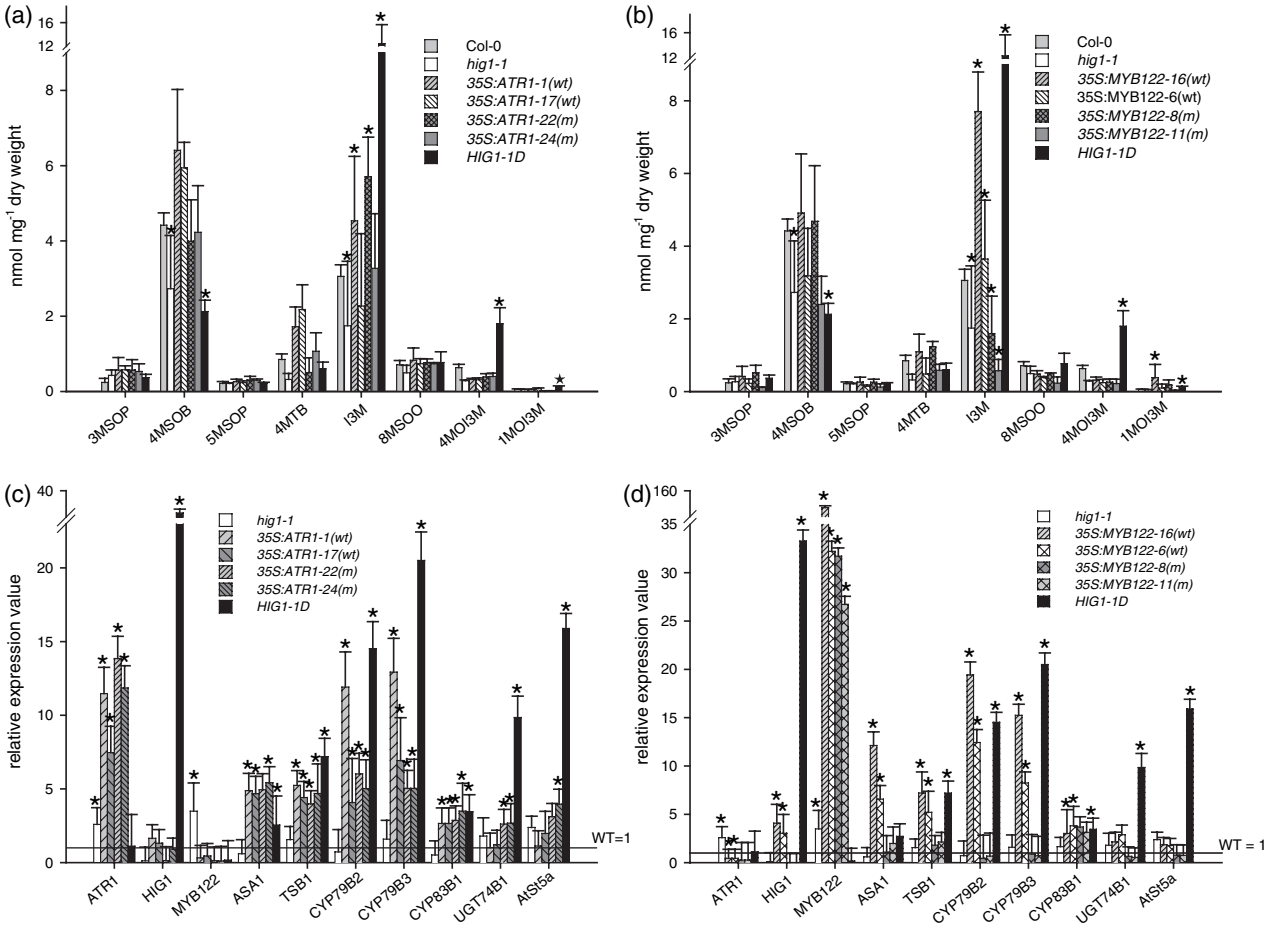

Figure 6. Glucosinolate contents and transcript levels of indolic glucosinolate pathway genes in rosette leaves of 5-week-old ATR1/MYB34 and MYB122 overexpression plants.

(a), (b) Glucosinolate contents (GS) in *hig1-1*, *ATR1*/*MYB34* and *MYB122* overexpressing lines. For comparison, the glucosinolate contents in the wild-type and *HIG1-1D* are also shown. *35S:ATR1-1(wt)* and *35S:ATR1-17(wt)*, wild-type background; *35S:ATR1-22(m)* and *35S:ATR1-24(m)*, *hig1-1* background. *35S:MYB122-16(wt)* and *35S:MYB122-6(wt)*, wild-type background; *35S:MYB122-8(m)* and *35S:MYB122-11(m)*, *hig1-1* background. 3MSOP, 3-methylsulfinylpropyl-GS; 4MSOB, 4-methylsulfinylbutyl-GS; 5MSOP, 5-methylsulfinylpentyl-GS; 4MTB, 4-methylthiobutyl–GS; I3M, indol-3-yl-methyl-GS; 8MSOO, 8-methylsulfinyloctyl-GS; 4MOI3M, 4-methoxyindol-3-ylmethyl-GS; 1MOI3M, 1-methoxyindol-3-ylmethyl-GS. Means ± SD, $n = 3$.

(c), (d) Real-Time RT-PCR analysis of indolic glucosinolate pathway genes measured in the overexpression lines *35S:ATR1-1(wt)*, *35S:ATR1-22/24(m)*, *35S:MYB122-16(wt)* and *35S:MYB122-8/11(m)*. For comparison, the gene expression levels in *hig1-1* and *HIG1-1D* are also presented. Relative gene expression values in comparison with the wild-type are shown (WT = 1). Means ± SD, $n = 3$). For details, see Experimental procedures.

*Significantly different (Student's *t* test; $P < 0.05$) in comparison with the wild-type.

indolic glucosinolate biosynthesis, *HIG1*/*MYB51* expression was analyzed in response to mechanical stimuli like wounding or touch. As shown in Figure 8a, mechanical puncturing already induced an increase in *HIG1*/*MYB51* gene expression in the wounded rosette leaves within 10 min, reaching a maximum after 30 min and fading away after 1 h, suggesting a transient response of *HIG1*/*MYB51* to mechanical stimuli. Remarkably, expression of *ATR1*/*MYB34* did not respond at all to wounding, and the induction of *MYB122* expression was observed only after a delay of about 1 h.

The activity of the *HIG1*/*MYB51* promoter in response to touch was analyzed in more detail using the *HIG1*/*MYB51*-promoter GUS reporter lines. As shown in Figure 8 (b–g), adult rosette leaves showed strong GUS staining at the position of the touch stimulus. Furthermore, we could observe intense GUS staining at the cutting sites of samples, including leaves and stems. These data suggest that *HIG1*/*MYB51* expression is induced in response to mechanical stimuli and might respond in a similar way to herbivore attack.

HIG1/*MYB51* overexpression reduces leaf consumption by a generalist herbivore

The breakdown of glucosinolates by myrosinase upon tissue damage is known as a defence mechanism against herbivores (Rask *et al.*, 2000; Mithen, 2001; Martin and Müller, 2007). As *HIG1*/*MYB51* expression is induced by mechanical stimuli and *HIG1*/*MYB51* overexpressing lines

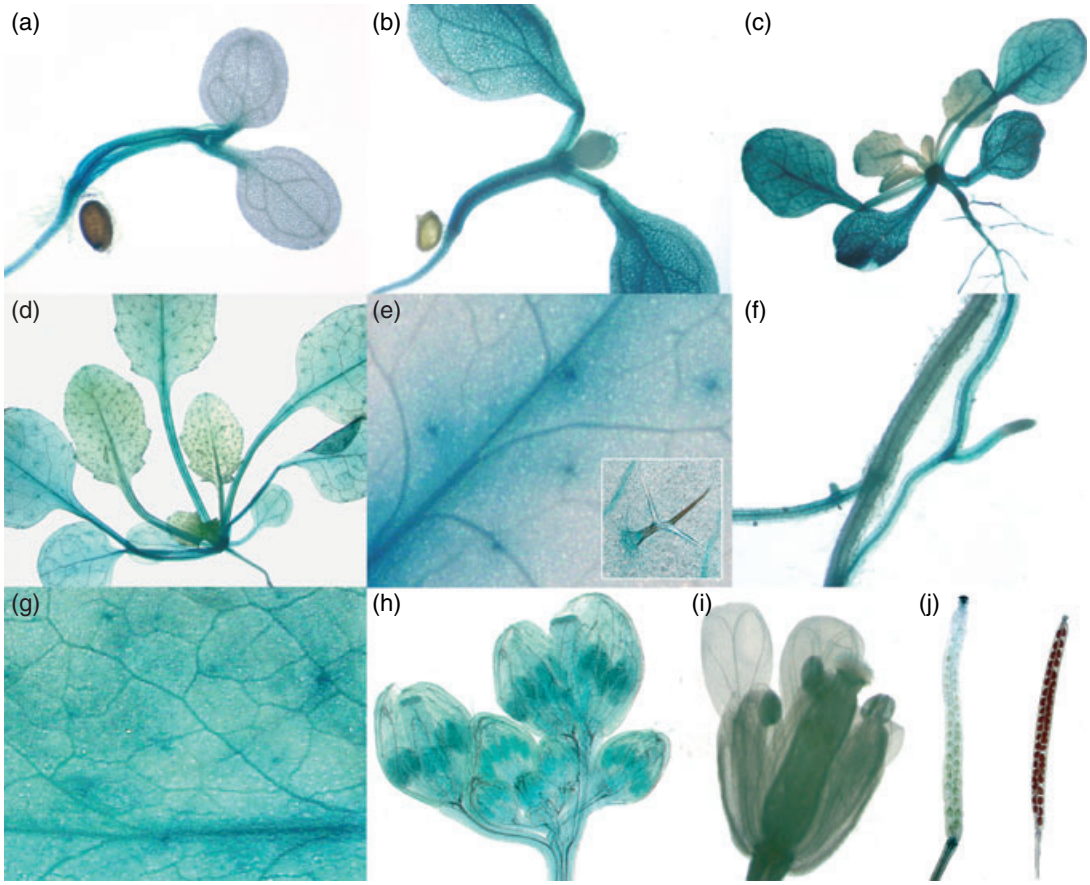

Figure 7. Histochemical GUS staining in tissues of Pro_{HIG1}:*GUS* plants:
(a) 3-day-old seedling;
(b) 14-day-old seedling;
(c) 3-week-old plant;
(d) 5-week-old plant;
(e) adult leaves (GUS expression in midvein and trichomes);
(f) roots of adult plants;
(g) fully expanded leaf;
(h) immature flower;
(i) mature flower;
(j) developing and mature siliques.

accumulate high levels of indolic glucosinolates, one can speculate about the role of HIG1/MYB51 in the plant defence system. To test this hypothesis, we assayed the consumption preference of the generalist lepidopteran herbivore *Spodoptera exigua* (Lepidoptera: Noctuidae) in dual-choice assays, measuring the leaf area consumed by fourth-instar larvae (n = 20 for each assay) maintained on an artificial diet before testing. When offering wild-type leaves and leaves of the *hig1-1* mutant, there was no feeding preference towards one of the lines, i.e. similar quantities of leaves from both lines were consumed (Figure 9). However, when leaves of the *HIG1-1D* overexpressor were offered together with wild-type or *hig1-1* mutant leaves, the larvae consumed significantly lower quantities of high indolic glucosinolate leaves (*HIG1-1D*) than of the other leaves offered. This clearly shows that *HIG1/MYB51* overexpression linked to a high indolic glucosinolate chemotype can increase plant resistance against generalist herbivores, and suggests a role of HIG1/MYB51 in plant defence against biotic challenges.

Discussion

HIG1/MYB51 *is a regulator of glucosinolate biosynthetic pathways*

Substantial progress has been achieved in the understanding of glucosinolate biosynthesis using forward and reverse genetics in the model plant *A. thaliana*. However, little is known about underlying regulatory mechanisms and genes

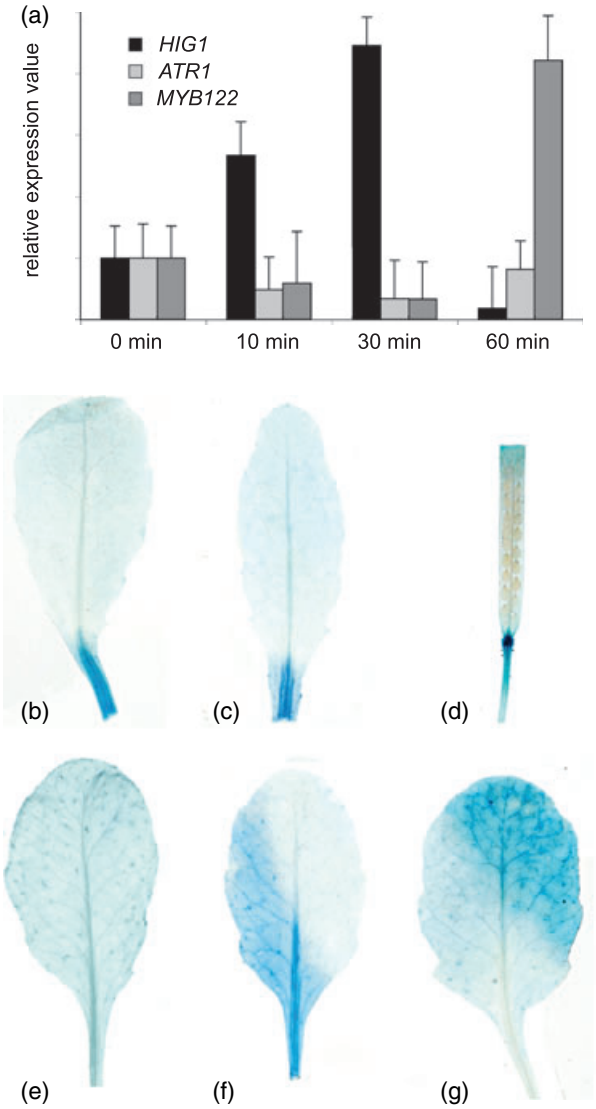

Figure 8. Induction of *HIG1*/*MYB51* expression by mechanical stimuli such as touch and wounding in fully expanded leaves, senescent leaves and siliques.
(a) Real-time RT-PCR analysis of *HIG1*/*MYB51*, *ATR1*/*MYB34* and *MYB122* gene expression upon wounding. Rosette leaves of 4–5-week-old plants were punctured and harvested at the indicated time points. Total RNA was reverse transcribed into cDNA and used as a template for quantitative RT-PCR as described in Experimental procedures; *Actin2* primers were used as control. Relative gene expression values are shown compared with non-wounded leaves (0 min = 1). Data are mean values ± SD of three individual experiments (n = 3).
(b to d) Induction of GUS expression in Pro_{HIG1}:*GUS* plants at the cutting sites.
(e to g) Induction of GUS expression in Pro_{HIG1}:*GUS* plants at the touch site. For details, see Experimental procedures.
(e) Untouched fully expanded leaf.
(f), (g) Different touch sites in fully expanded leaf.

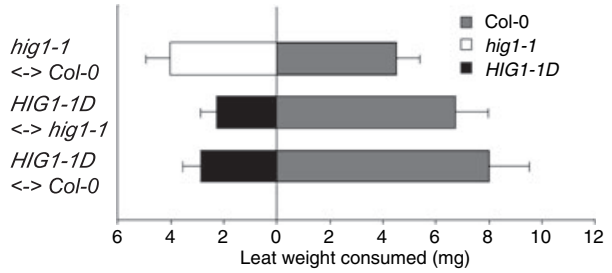

Figure 9. Dual-choice assay with the generalist herbivore *Spodoptera exigua*. The graph shows the preference (mean leaf consumption in FW ± SD) of larvae for leaves from either wild-type (Col-0) and *hig1-1* loss-of-function mutant (n = 20; P = 0.757) (upper bar), *HIG1-1D* gain-of-function and *hig1-1* loss-of function mutants (n = 20; P = 0.0113) (middle bar) and *HIG1-1D* gain-of-function and wild-type (n = 20; P = 0.0026) (lower bar). P values calculated using Student's t tests show significant avoidance of the high-indolic glucosinolate line *HIG1-1D*.

that coordinate and control glucosinolate compound accumulation during development and in response to environmental challenges. Recently, the first regulatory factors involved in the control of glucosinolate biosynthesis, including IQD1 were described (Levy *et al.*, 2005; see Introduction). In addition, the R2R-MYB transcription factor ATR1/MYB34, which is known to activate tryptophan biosynthetic genes (Bender and Fink, 1998), has been reported to act as a regulator of indolic glucosinolate homeostasis (Celenza *et al.*, 2005).

Here, we present HIG1/MYB51 as a new regulator of glucosinolate biosynthesis identified as an activation-tagged mutant (*HPC1-1D, HIG1-1D*), that was initially isolated in a screen for mutants with altered accumulation of secondary metabolites (Schneider *et al.*, 2005). The chemotype caused by the dominant *HIG1-1D* allele, namely the accumulation of I3M, was shown to be caused by *4x35S* enhancer-mediated overexpression of the R2R3-MYB transcription factor *HIG1*/*MYB51*. *4x35S* enhancer elements have been demonstrated to increase quantitatively the original expression pattern of a gene, and not to lead to constitutive overexpression (Neff *et al.*, 1999; van der Graaff *et al.*, 2003). Remarkably, ectopic overexpression of *HIG1*/*MYB51* in the wild-type background could phenocopy the chemotype of the original activation-tagged line *HIG1-1D* (Figure 2). On the other hand, a T-DNA insertion allele of *HIG1*/*MYB51* (*hig1-1*) caused a significant reduction in I3M levels, and this chemotype could be counteracted by overexpression of *HIG1*/*MYB51* (Figure S3). Thus, HIG1/MYB51 represents an important, but certainly not the only, regulatory component controlling indolic glucosinolate biosynthesis in *A. thaliana*. Notably, neither the *hig1-1* mutant nor the *HIG1-1D* or *HIG1*/*MYB51* overexpressing plants showed significant changes in IAA levels or aberrant growth phenotypes indicative for distorted auxin levels (Figure 5).

We also demonstrate that genes involved in the biosynthesis of tryptophan and indolic glucosinolate biosynthesis, i.e. *DHS1*, *TSB1*, *CYP79B2*, *CYP79B3*, *CYP83B1* and *AtST5a*, are activated by HIG1/MYB51 in *trans* (Figure 4). Thus, HIG1/MYB51 appears to serve as a general activator of both

tryptophan synthesis genes and tryptophan secondary metabolism genes. A co-regulation of indolic glucosinolate pathway enzymes and tryptophan biosynthetic enzymes has been observed by analyzing microarray data derived from different stress experiments (Gachon *et al.*, 2005). Hence, the activation of the tryptophan biosynthetic pathway seems to be required for providing sufficient levels of the precursor tryptophan for the increased formation of indolic glucosinolates in response to stress.

The level of the main short-chain aliphatic glucosinolate 4MSOB is lower in *HIG1-1D* and in *HIG1*/*MYB51* overexpression lines compared with the wild-type (Figures 2 and 6). It thus appears that *HIG1*/*MYB51* possesses opposite effects on the biosynthetic pathways of indolic and aliphatic glucosinolates. One may speculate that the decreased accumulation of methionine-derived glucosinolates may result from a metabolic crosstalk between both branches of glucosinolate biosynthesis, by which a distinct ratio of the different glucosinolates is maintained. The 'limiting electron hypothesis', which has been recently proposed, could serve as an explanation for these observations (Grubb and Abel, 2006): the competition of cytochrome P450 monooxygenases involved in aliphatic (CYP79F1, CYP79F2 and CYP83A1) and indolic glucosinolate (CYP79B2, CYP79B3 and CYP83B1) biosynthetic pathways for electrons to reduce dioxygen to water could be the reason for a reciprocal negative feedback regulation between both branches of glucosinolate biosynthesis.

Strikingly, the *hig1-1* null allele caused not only reduced levels of indolic glucosinolates, but also of short-chain aliphatic glucosinolates, resulting in a reduction of the total glucosinolate content by approximately 65% (Figure 2). On the other hand, *HIG1*/*MYB51* overexpression in both the wild-type and the *hig1-1* mutant background led to the expected increase in the level of indolic glucosinolates, with aliphatic glucosinolates remaining at low levels (Figure 2; Figure S3). The reason for this is not known yet but might point to a regulatory interplay between HIG1/MYB51 and other factors involved in the control of both indolic and aliphatic glucosinolate biosynthetic genes. It is feasible, for example, that the activity of putative regulators of aliphatic glucosinolate biosynthesis and corresponding biosynthetic genes is altered in the *hig1-1* mutant.

Roles of HIG1/MYB51*,* ATR1/MYB34 *and* MYB122 *in the regulation of glucosinolate biosynthesis are divergent*

A. thaliana mutants defective in the early steps of the glucosinolate biosynthetic pathway, or overexpressing these enzymes, all show an altered morphology reminiscent of IAA overexpression or IAA repression phenotypes, respectively (Zhao *et al.*, 2002; Barlier *et al.*, 2000; Bak *et al.*, 2001; Reintanz *et al.*, 2001). These observations can be attributed to the fact that IAOx as a product of CYP79B2 and CYP79B3 actions is an important intermediate of both the indolic glucosinolate and IAA pathways (Figure 3). Overexpression of the transcription factor *AtDof1.1* causes changes in glucosinolate profiles, but also affects auxin accumulation (Skirycz *et al.*, 2006). Overexpression of *ATR1*/*MYB34* was shown earlier to result in a hyperactivation of indolic glucosinolate pathway genes, accompanied by only a modest elevation of IAA levels with no impact on plant growth (Celenza *et al.*, 2005).

The question of how glucosinolate biosynthesis is regulated (for example, in response to biotic stresses) without a strong impact on auxin biosynthesis is still open. It does not appear implicitly favourable to plants to alter IAA biosynthesis when an increased biosynthesis of indolic glucosinolates is required. Our data demonstrate that even though both IAA and indolic glucosinolate biosynthetic pathways share common enzymes, both pathways can be specifically regulated to allow appropriate plant responses to environmental challenges. HIG1/MYB51 can activate genes both upstream and downstream of IAOx, leading to increased indolic glucosinolate levels without a significant effect on IAA contents (Figures 2, 5b and 6). Even though ATR1/MYB34 can partially rescue the low-indolic glucosinolate *hig1-1* mutant chemotype, overexpression of *ATR1*/*MYB34* in the *hig1-1* or wild-type background in our hands led to up to sevenfold higher IAA levels, reflected by pronounced high-IAA growth phenotypes (Figure 5a). In addition, all *ATR1*/*MYB34* overexpressing plants were defective in the development of generative organs, the root system, as well as the vegetative biomass. In contrast, *HIG1*/*MYB51* overexpressors and *hig1-1* plants display unaltered morphology compared with the wild-type, and also the IAA levels of these plants are, if at all, only slightly altered (Figure 5).

Remarkably, *ASA1* is not *trans*-activated by HIG1/MYB51 (Figure 4), and the upregulation of *ASA1* therefore does not seem to be required for an increased biosynthesis of indolic glucosinolates. However, ASA1 appears to play a pivotal role in the regulation of auxin biosynthesis. For example, the ethylene-triggered activation of auxin biosynthesis was recently shown to be strictly dependent on ASA1. Likewise, the high-IAA phenotype of *sur1* and *sur2* mutants with defects in C-S lyase and CYP83B1 functions, respectively, is suppressed in mutants defective in ASA1/WEI2 function (Stepanova *et al.*, 2005). Also, these results support the hypothesis that *ATR1*/*MYB34* overexpression, which does cause increased steady-state levels of *ASA1* transcripts (Celenza *et al.*, 2005; Figure 6c), might primarily be linked to the regulation of IAA homeostasis.

In addition, the observation that *ATR1*/*MYB34* does not show any expression in vegetative parts of the plant, e.g. rosette leaves, argues against a major role of ATR1/MYB34 in the control of indolic glucosinolate biosynthesis in leaves of adult plants (Figure S5; AtGenExpress data

analyzed using Genevestigator, http://www.genevestigator.ethz.ch/).

In contrast to *ATR1*/*MYB34*, *MYB122* could not rescue the low-indolic glucosinolate chemotype of the *hig1-1* mutant (Figure 6b). Likewise, *MYB122* overexpression did not cause a high-IAA phenotype in *hig1-1* mutants, which raises the question about the role of MYB122 in the tryptophan pathway. Overexpression of *MYB122* in the wild-type background, however, led to the enhanced transcription of several tryptophan pathway genes, including *ASA1*, *TSB1*, *CYP79B2*, *CYP79B3* and *CYP83B1*, along with elevated auxin levels (Figures 5b and 6). A number of scenarios may explain this result. Increased IAA production could cause a positive feedback on the expression of these genes. Alternatively, MYB122 could directly enhance the expression of these genes, although only in concert with HIG1/MYB51. In addition, or alternatively, HIG1/MYB51 and/or MYB122 could act as activators or repressors, depending on the context, in a similar way as it has been shown for MYB4 (Jin *et al.*, 2000).

It can be concluded that ATR1/MYB34, HIG1/MYB51 and MYB122 apparently have different roles in the regulation of indolic glucosinolate and IAA biosynthetic pathways. All three factors have the potential to upregulate glucosinolate biosynthetic pathway genes, e.g. *TSB1*, *CYP79B2* and *CYP79B3*, and can positively regulate indolic glucosinolate accumulation. However, along with increased levels of indolic glucosinolates, overexpression of *ATR1*/*MYB34* and *MYB122* led to high-IAA phenotypes. Only the overexpression of *HIG1*/*MYB51* led additionally to the activation of genes further downstream of *CYP83B1*, i.e. of *UGT74B1* and *AtST5a*. These plants did not exhibit an aberrant growth phenotype. Obviously, the next step is a detailed analysis of the interplay of subgroup 12 R2R3-MYB factors, and potentially other factors, in controlling distinct but partially overlapping sets of target genes from IAA and glucosinolate biosynthetic pathways.

HIG1/MYB51 *is expressed at sites of indolic glucosinolate accumulation and plays a role in biotic stress responses*

The expression of glucosinolate biosynthetic genes in *A. thaliana*, e.g. that of *CYP79B2*, *UGT74B1*, *CYP79F1* and *CYP79F2*, and also of recently discovered regulators of glucosinolate biosynthesis, *IQD1* and *AtDof1.1*, often appeared to be restricted to vascular tissues (Mikkelsen *et al.*, 2000; Grubb *et al.*, 2004; Reintanz *et al.*, 2001; Levy *et al.*, 2005; Skirycz *et al.*, 2006). *HIG1*/*MYB51* expression overlaps with the expression of these genes but, in addition, is also present in the mesophyll of mature rosette leaves, the pavement cells of young rosette leaves and trichomes (Figure 7). Thus, *HIG1*/*MYB51* expression correlates at least to a great extent with the sites of indolic glucosinolates biosynthesis and accumulation, an observation that is in accordance with the role of *HIG1*/*MYB51* as a positive regulator of this pathway.

Environmental stimuli such as herbivore attack or wounding are known to have a great impact on the regulation of glucosinolate biosynthesis. Several glucosinolate biosynthetic pathway genes were shown to be induced upon mechanical stimuli or hormone treatment (Brader *et al.*, 2001; Kliebenstein *et al.*, 2002b; Mikkelsen *et al.*, 2003; Mewis *et al.*, 2005). Here we show that expression of *HIG1*/*MYB51*, but not of ATR1/MYB34, in leaves is rapidly induced by wounding or touch (Figure 8). It is tempting to speculate that HIG1/MYB51 is a key player in the signal transduction chain leading from the touch perception output to an increased biosynthesis of indolic glucosinolates, thereby rendering the plant more resistant to herbivores. It could indeed be shown that generalist herbivores avoided the *HIG1-1D* line with higher contents of indolic glucosinolates in dual-choice assays (Figure 9). Furthermore, QTL (quantitative trait locus) mapping analyses in *A. thaliana* (Kliebenstein *et al.*, 2002a) provided data concerning a QTL controlling herbivore resistance in a L*er* × Col population, which could be mapped on chromosome I between 14 and 28 cM. This QTL nicely fits to the position of the locus At1g18570 encoding *HIG1*/*MYB51*. This finding adds further evidence to the assignment of HIG1/MYB51 as an important regulatory component in controlling glucosinolate biosynthesis upon biotic challenges.

Until now it was assumed that the common pathway for the biosynthesis of both IAA and indolic glucosinolates in plants from the Brassicaceae family is simultaneously regulated by ATR1/MYB34. As shown in this study, HIG1/MYB51 obviously represents a key component in controlling the mechanical-induced regulation of the indolic glucosinolate biosynthetic pathway in *A. thaliana* without affecting IAA biosynthesis and plant morphology.

Experimental procedures

Plant materials and growth conditions

Plants (*A. thaliana* ecotype Columbia) were grown in a temperature-controlled greenhouse under a 16-h light/8-h dark regime or in a growth chamber under a 12-h light/12-h dark regime at day/night temperatures of 21°C/18°C and at 40% humidity. The *HIG1-1D* activation-tagged mutant was previously identified as *HPC1-1D* in a population of activation-tagged lines (Schneider *et al.*, 2005). The *hig1-1* line GK-228B12 is homozygous for a T-DNA insertion in the second exon of *HIG1*/*MYB51*, and was supplied by GABI-Kat (Rosso *et al.*, 2003); the *HIG1*/*MYB51* transcript is not detectable in *hig1-1* plants (see Figure 2a).

Preparation of methanolic extracts and HPLC analysis of desulfoglucosinolates

Leaves (50–80 mg) were placed in a 1.5-mL reaction tube and frozen in liquid nitrogen. Frozen leaf samples were lyophilized and homogenized in a mill (MM301; Retsch, http://www.retsch.com). Glucosinolates were extracted in 80% methanol after the addition of

20 μl of a 5 mM solution of benzyl glucosinolate (http://www.glucosinolates.com) as an internal standard. Extracts were loaded on a DEAE Sephadex A25-column (0.1 g powder equilibrated in 0.5 M acetic acid/NaOH, pH 5). Glucosinolate analysis was performed by conversion to desulfoglucosinolates through overnight incubation with purified sulfatase (EC 3.1.6.1) designated 'type H-1, from *Helix pomatia*, 16 400 U g^{-1} solid' (Sigma, http://www.sigmaaldrich.com). For analysis of desulfo glucosinolates, samples were subjected to HPLC analysis on a 1100 Series chromatograph (Hewlett-Packard, http://www.hp.com) with a quaternary pump and a 1040M diode-array detector. Elution was accomplished on a Supelco C-18 column (Supelcosil LC-18, 250 × 4.6 mm, 5 μm; Supelco, http://www.sigmaaldrich.com/Brands/Supelco_Home.html) with a gradient (solvent A, water; solvent B, methanol) of 0–5% B (10 min), 5–38% B (24 min), followed by a cleaning cycle (38–100% B in 4 min, with a 6-min hold, then 100–0% B in 5 min, with a 7-min hold). Peaks were quantified by the peak area at 229 nm (bandwidth 4 nm) relative to the area of the internal standard peak, applying the response factors as described by Brown *et al.* (2003).

Construction of transgenic recapitulation A. thaliana *plants and constructs for* ATR1/MYB34 *and* MYB122 *overexpression*

To generate *HIG1*/*MYB51* overexpression (recapitulation) plants, the *HIG1*/*MYB51* full-length coding sequence (without the stop codon) was amplified by RT-PCR and cloned into the Entry TOPO vector (Invitrogen, http://www.invitrogen.com). For primer sequences, see Table S1. To drive expression of the *HIG1*/*MYB51* coding sequence under control of the *CaMV 35S* promoter, the binary Gateway compatible plant transformation vector pGWB2 was used. To recombine the insert from the entry clone into the destination vector, an LR reaction (Invitrogen) between both clones was performed. The final *35S:HIG1:pGWB2* construct was transformed into *Agrobacterium tumefaciens* (strain GV3101) by electroporation and into *A. thaliana* plants by vacuum infiltration.

To complement the *hig1-1* loss-of-function mutant with the *ATR1*/*MYB34 and MYB122* genes, the *ATR1*/*MYB34* and MYB122 full-length coding sequences were amplified by RT-PCR and cloned into the Entry TOPO vector (for primer sequences, see Table S1). To recombine the insert from the entry clone into the destination vector, an LR reaction between the Entry vectors containing *ATR1*/*MYB34* and *MYB122*, and the *pGWB2* destination vector were performed. The final *35S:ATR1:pGWB2 and 35S:MYB122:pGWB2* constructs were transformed into *A. tumefaciens* (strain GV3101) by electroporation, and finally into *A. thaliana* wild-type and the *hig1-1* mutant by vacuum infiltration. All transformants were selected with kanamycin and verified by PCR analysis. At least 70 independent primary transformants were analyzed by RT-PCR.

Histochemical analysis of transgenic plants expressing the Pro_{HIG1}*:uidA fusion construct: wounding and touch treatments*

The *HIG1*/*MYB51*-promoter region (from −1676 to + 342 bp) was amplified from genomic DNA of *A. thaliana* plants and cloned into the Entry TOPO vector (Invitrogen) (for primer sequences, see Table S1). To drive expression of *uidA* under control of the *HIG1*/*MYB51* promoter, the binary Gateway compatible plant transformation vector pGWB3 was recombined with the Topo Entry vector using an LR reaction. The Pro_{HIG1}*:uidA* clone in pGWB3 was used to transform *A. tumefaciens* and *A. thaliana*.

Transformants were selected with kanamycin and verified by PCR analysis. Histochemical localization of GUS in transgenic plants harbouring the Pro_{HIG1}*:uidA* construct was performed as described by Jefferson *et al.* (1987) with some modifications. Sample tissues were infiltrated with the reaction buffer [50 mM Na_2HPO_4-NaH_2PO_4, pH 7.0, 0.5 mM $K_3Fe(CN)_6$, 0.5 mM $K_4Fe(CN)_6$, containing 2 mM 5-bromo-4-chloro-3-indolyl-β-D-glucuronic acid (X-Gluc) as substrate] under vacuum and incubated at 37°C overnight. Plant pigments were destained with 80% ethanol, and the GUS staining patterns were recorded under a binocular microscope (SMZ-U; Nikon, http://www.nikon.com).

Wounding of plants involved the mechanical treatment of leaves by cutting with a scalpel followed by GUS staining. For the leaf touch experiments, pressure was exerted by gently pushing part of the leaf between thumb and forefinger. Approximately 50% of the leaf area was left untouched. After 3–10 min, leaves were collected and infiltrated for GUS staining. Control plants were carefully collected avoiding any kind of mechanical stimuli and were subjected to the same infiltration procedure.

Real-time PCR analysis

The expression of glucosinolate biosynthesis genes was analyzed by real-time quantitative RT-PCR analysis using the fluorescent intercalating dye SYBR-Green in a GeneAmp® 5700 Sequence Detection System (Applied Biosystems, http://www.appliedbiosystems.com). The Arabidopsis *ACTIN2* gene was used as a standard. A two-step RT-PCR analysis was performed. First, total RNAs (10 μg per reaction) were reversely transcribed into cDNAs, using the First-Strand cDNA Synthesis SSII Kit (Invitrogen) according to the manufacturer's instructions. Subsequently, the cDNAs were used as templates in real-time PCR reactions with gene-specific primers (Table S2). The real-time PCR reaction was performed using SYBR-Green master Kit System (Applied Biosystems) according to the manufacturer's instructions. The *C*t, defined as the PCR cycle at which a statistically significant increase of reporter fluorescence is detected, is used as a measure for the starting copy number of the target gene. Relative quantification of expression levels was performed using the comparative *C*t method (see manufacturer's instructions, Bulletin #2, Applied Biosystems). The relative value for the expression level of each gene was calculated by the equation $Y = 2^{-\Delta\Delta Ct}$, where ΔCt is the difference between control and target products ($\Delta Ct = Ct_{GENE} - Ct_{ACT}$,) and $\Delta\Delta Ct = \Delta Ct_{mutant} - \Delta Ct_{wt}$. Thus, the calculated relative expression values are normalized to the wild-type expression level, WT = 1. The efficiency of each primer pair was tested using wild-type (Col-0) cDNA as a standard template, and the RT-PCR data were normalized dependent on the relative efficiency of each primer pair.

Auxin measurements

For IAA analysis, about 200 mg of leaf material was collected, immediately frozen in liquid nitrogen and homogenized. Subsequently, 1 ml of methanol (60°C) containing 10 pmol ml^{-1} deuterated $[^2H]_2$-IAA was added and the sample was further homogenized. The samples were shaken at 20°C for 60 min and then centrifuged for 15 min at 20 000 × g. The supernatant was concentrated to dryness using a vacuum evaporator, and the further processing of samples and the subsequent quantitative analysis of IAA as its methyl ester by chemical ionization (methanol) gas-chromatography tandem-mass-spectrometry (GC-MS/MS) were

performed as described by Müller and Weiler (2000). All spectra were recorded on a Varian Saturn 2000 ion-trap mass spectrometer connected to a Varian CP-3800 gas chromatograph fitted with a CombiPal autoinjector (Varian, http://www.varianinc.com). The following mother ions were used for quantification: IAA, *m/z* = 190 $[M + H]^+$, $[^2H]_2$-IAA *m/z* = 192 $[M + H]^+$. The quantities of endogenous compounds were calculated from the signal ratios of the unlabelled daughter ion (*m/z* = 130) over the stable isotope-containing daughter ion (*m/z* = 132) for each sample (Müller and Weiler, 2000).

Effector and reporter construction for transient co-transformation experiments

Promoter regions of *DHS1* (from –1152 to + 351 bp), *ASA1* (from –1210 to + 96 bp), *TSB1* (from –2320 to + 132 bp), *CYP79B2* (from –1383 to + 81 bp), *CYP79B3* (from –1353 to + 84 bp), *CYP83B1* (from –995 to + 27 bp) and *AtST5a* (from –1134 to + 141 bp) genes were amplified from genomic DNA of *A. thaliana* plants. The corresponding primer sequences are listed in Table S1. Promoters of *Dsh1, ASA1, CYP79B2, CYP79B3, CYP83B1* and *AtST5a* genes were cloned into pEntry TOPO vector (Invitrogen). To drive Agrobacteria-mediated expression of *uidA* under control of those promoters, the binary plant transformation vector pGWB3i containing an intron within the GUS gene was generated. An 189-bp intron fragment was amplified from pPCV 6NFHyg GUS Int Vector (Vancanneyt *et al.*, 1990) using a proof-reading polymerase. The blunt-ended PCR product was ligated to pGWB3 using the *Sna*BI restriction site. Using LR reactions (Invitrogen), pGWB3i was recombined with the pEntry Topo vectors containing the different promoters. The final Pro_{DSH1}*:uidA*, Pro_{ASA1}*:uidA*, Pro_{TSB1}*:uidA*, $Pro_{CYP79B2}$*:uidA*, $Pro_{CYP79B3}$*:uidA*, $Pro_{CYP83B1}$*:uidA and* Pro_{AtST5a}*:uidA* clones in pGWB3i, as well as *35S:HIG1* in pGWB2, were used to transform the supervirulent *A. tumefaciens* strain LBA4404.pBBR1MCS.virGN54D.

Plant transfection via infiltration and fluorimetric GUS activity assay

To estimate the transactivation potential of *HIG1/MYB51* towards promoters of target genes, the supervirulent Agrobacteria containing 3*5S:HIG1* in pGWB2 (effector), the same strain containing the empty pGWB2, and the antisilencing Agrobacteria strain 19K (Voinnet *et al.*, 1999), and each of the reporter promoters in pGWB3i vector within the supervirulent Agrobacteria were taken from fresh YEB plates, grown overnight, sedimented, re-suspended in 10 mM $MgCl_2$, 10 mM 2-(*N*-morpholine)-ethanesulphonic acid (MES), pH 5.6, and adjusted to an OD of 0.7–0.8. Two working solutions were prepared for each promoter and at least six plants were infiltrated. Working solution 1 contained a suspension with effector and reporter constructs together with the Agrobacteria strain 19K in a 1:1:1 ratio. Working solution 2 contained a suspension with an empty vector (without effector), reporter and 19K Agrobacteria strain in a 1:1:1 ratio. Acetosyringon was added (0.15 mM, final concentration) and the suspension was incubated for 2–4 h at room temperature.

Leaves of three plants were infiltrated with each working solution using a syringe. Following infiltration, plants were exposed for 12–24 h in darkness. Either five or six leaf probes were taken randomly from infiltrated plants for protein isolation and GUS activity measurements after 4 days of transient expression.

One part of the transfected leaf was subjected to histochemical staining and the other part to fluorimetric determination of GUS activity. Quantitative fluorimetric GUS assays were performed using 4-methylumbelliferyl-β-glucuronide (MUG) as a substrate dissolved in 50 mM sodium phosphate buffer (pH 7), 1 mM EDTA and 0.1% Triton X-100, as described by Jefferson *et al.* (1987). Protein content was determined using the BCA kit (Pierce Biotechnology, http://www.piercenet.com) and bovine serum albumin as a standard. The activity of the reporter gene was expressed in nmol 4-methylumbelliferone (4-MU) per min and mg of extracted protein.

Dual-choice assays

Dual-choice assays were performed to study the consumptional preference of the generalist lepidopteran herbivore, *S. exigua* (Lepidoptera: Noctuidae). Eggs of *S. exigua* were received from Bayer CropScience (http://www.bayercropscience.com) and larvae were maintained on an artificial diet. Fourth-instar larvae were used in dual-choice assays. Larvae were tested individually in Petri dishes (5.5 cm in diameter), offering them two leaves of equivalent age of different Arabidopsis lines on moistened filter paper for 8 h at 25°C. Leaves were weighed and scanned before and after feeding. Leaf area was analyzed using Winfolia (Regent Instruments Inc., http://www.regent.qc.ca). Three different pair combinations of leaves were provided to each of 20 larvae: *HIG1-1D* and wild-type (Col-0), *HIG1-1D* and *hig1-1,* and Col-0 and *hig1-1*. The consumed FW was calculated using the following: [(weight begin*area end)/area begin].

Acknowledgements

We thank Professor E. Weiler (University Bochum, Germany) for IAA determinations, B. Kleinhenz for excellent technical assistance and R. Yatusevich for cloning promoter GUS constructs used in the co-transformation assays. The Gateway destination vectors used in this work (pGWB2, pGWB3 and pGWB5) were kindly provided by T. Nakagawa (Shimane University, Japan). Eggs of *Spodoptera exigua* were received from Bayer CropScience (Monheim, Germany). This work was supported by grants from the European Union (QLK1-CT-2001-01 080), the Deutsche Forschungsgemeinschaft and the Fonds der Chemischen Industrie.

Supplementary material

The following supplementary material is available for this article online:

Figure S1. Overexpression of *HIG1/MYB51* results in the accumulation of glucobrassicin.

Mass spectrum of the compound purified from the *HIG1-1D* mutant. The most intensive ion observed was *m/z* = 369.09 consistent with the structural formulae of $C_{16}H_{20}N_2O_9S_2$ for glucobrassicin. The presence of two nitrogen atoms was confirmed by labelling of plants with ^{15}N-medium.

Figure S2. HIG1/MYB51 is localized to the cell nucleus.

Subcellular localization of a Pro_{35S}*:HIG1:GFP* translational fusion in BY2 tobacco protoplasts (a to c), cultured *A. thaliana* cells (d to f), and transiently transformed *A. thaliana* rosette leaves (g and h).

(a) The Pro_{35S}*:HIG1:GFP* construct is localized to the nucleus.

(b) DAPI staining of the nucleus.

(c) GFP distribution in the cytoplasm (empty vector).

(d) Pro_{35S}*:HIG1:GFP* fluorescence.

(e) DAPI staining of the nucleus.
(f) Brightfield image and GFP fluorescence.
(g) *Pro$_{35S}$:HIG1:GFP* fluorescence.
(h) DAPI staining of nuclei.

Figure S3. Overexpression of *HIG1/MYB51* in the *hig1-1* mutant background.

(a) Growth phenotypes of *hig1-1* mutants transformed with *35S:HIG1*. Two representative independent transgenic lines *35S:HIG1-A(m)* and *35S:HIG1-A(m)* are shown with growth phenotypes comparable to that of the wild-type (Col-0) and the *hig-1-1* mutant.

(b) The transformed plants possess higher levels of indolic glucosinolates and a lower level of the aliphatic glucosinolate 4MSOB as it is the case for *HIG1-1D* and *35S:HIG1* plants, overexpressing *HIG1/MYB51* in the wild-type background.

Figure S4. Transcript levels of *NITRILASE 2* in *HIG1/MYB51*, *ATR1/MYB34*, and *MYB122* overexpression lines as measured by real-time RT-PCR.

ATR1/MYB34 overexpressing plants (Col-0 background) show a dramatic increase in the expression of the *NITRILASE 2* gene. Relative gene expression values in comparison with the wild-type (WT = 1).

Figure S5. Histochemical GUS staining in tissues of *Pro$_{ATR1}$:GUS* plants.

Three different promoter fragments varying from 1.5 kb to 3.6 kb in length of the *ATR1/MYB34* gene have been used for the generation of transgenic *Pro$_{ATR1}$:GUS* plants. About 20 independent transgenic lines have been analyzed in detail. All of them show similar GUS expression patterns.

(a) Absence of GUS staining in rosette leaves.
(b) GUS staining in mature flowers and meristematic tissue of growing inflorescences.
(c) Stamen.
(d) Inflorescences and immature flowers.
(e) GUS staining in the meristematic tissue of generative organs.

Table S1 Primers used for the amplification of genes and generation of constructs.

Table S2 Primers used for real-time RT-PCR.

This material is available as part of the online article from http://www.blackwell-synergy.com

References

Bak, S. and Feyereisen, R. (2001) The involvement of two P450 enzymes, CYP83B1 and CYP83A1, in auxin homeostasis and glucosinolate biosynthesis. *Plant Physiol.* **127**, 108–118.

Bak, S., Tax, F.E., Feldmann, K.A., Galbraith, D.W. and Feyereisen, R. (2001) CYP83B1, a cytochrome P450 at the metabolic branch point in auxin and indole glucosinolate biosynthesis in Arabidopsis. *Plant Cell*, **13**, 101–111.

Barlier, I., Kowalczyk, M., Marchant, A., Ljung, K., Bhalerao, R., Bennett, M., Sandberg, G. and Bellini, C. (2000) The SUR2 gene of *Arabidopsis thaliana* encodes the cytochrome P450CYP83B1, a modulator of auxin homeostasis. *Proc. Natl. Acad. Sci. USA*, **97**, 14819–14824.

Bartel, B. and Fink, G.R. (1994) Differential expression of auxin producing gene family in *Arabidopsis thaliana*. *Proc. Natl. Acad. Sci. USA*, **91**, 6649–6653.

Bednarek, P., Schneider, B., Svatos, A., Oldham, N.J. and Hahlbrock, K. (2005) Structural complexity, differential response to infection, and tissue specificity of indolic and phenylpropanoid secondary metabolism in Arabidopsis roots. *Plant Physiol.* **138**, 1058–1070.

Bender, J. and Fink, G.R. (1998) A Myb homologue, ATR1, activates tryptophan gene expression in Arabidopsis. *Proc. Natl Acad. Sci. USA*, **95**, 5655–5660.

Brader, G., Tas, E. and Palva, E.T. (2001) Jasmonate-dependent induction of indole glucosinolates in Arabidopsis by culture filtrates of the nonspecific pathogen *Erwinia carotovora*. *Plant Physiol.* **126**, 849–860.

Brown, P.D., Tokuhisa, J.G., Reichelt, M. and Gershenzon, J. (2003) Variation of glucosinolate accumulation among different organs and developmental stages of *Arabidopsis thaliana*. *Phytochemistry*, **62**, 471–481.

Celenza, J.L., Quiel, J.A., Smolen, G.A., Merrikh, H., Silvestro, A.R., Normanly, J. and Bender, J. (2005) The Arabidopsis ATR1 Myb transcription factor controls indolic glucosinolate homeostasis. *Plant Physiol.* **137**, 253–262.

Gachon, C.M.M., Langlois-Meurinne, M., Henry, Y. and Saindrenan, P. (2005) Transcriptional co-regulation of secondary metabolism enzymes in Arabidopsis: functional and evolutionary implications. *Plant Mol. Biol.* **58**, 229–245.

van der Graaff, E., Nussbaumer, C. and Keller, B. (2003) The *Arabidopsis thaliana rlp* mutations revert the ectopic leaf blade formation conferred by activation tagging of the *LEP* gene. *Mol. Genet. Genomics*, **270**, 243–252.

Gross, H.B., Dalebout, T., Grubb, C.D. and Abel, S. (2000) Functional detection of chemopreventive glucosinolates in *Arabidopsis thaliana*. *Plant Sci.* **159**, 265–272.

Grsic-Rausch, S., Kobelt, P., Siemens, J.M., Bischoff, M. and Ludwig-Müller, J. (2000) Expression and localisation of nitrilases during symptom development of the clubroot disease in Arabidopsis. *Plant Physiol.* **122**, 369–378.

Grubb, C.D. and Abel, S. (2006) Glucosinolate metabolism and its control. *Trends Plant Sci.* **11**, 89–100.

Grubb, C.D., Zipp, B.J., Ludwig-Muller, J., Masuno, M.N., Molinski, T.F. and Abel, S. (2004) Arabidopsis glucosyltransferase UGT74B1 functions in glucosinolate biosynthesis and auxin homeostasis. *Plant J.* **40**, 893–908.

Jefferson, R.A., Kavanagh, T.A. and Bevan, M.W. (1987) GUS Fusions: beta-glucuronidase as a sensitive and versatile gene fusion marker in higher plants. *EMBO J.* **6**, 3901–3907.

Jin, H., Cominelli, E., Bailey, P., Parr, A., Mehrtens, F., Jones, J., Tonelli, C., Weisshaar, B. and Martin, C. (2000) Transcriptional repression by AtMYB4 controls production of UV-protecting sunscreens in *Arabidopsis*. *EMBO J.* **19**, 6150–6161.

Kliebenstein, D.J., Kroymann, J., Brown, P., Figuth, A., Pedersen, D., Gershenzon, J. and Mitchell-Olds, T. (2001) Genetic control of natural variation in Arabidopsis glucosinolate accumulation. *Plant Physiol.* **126**, 811–825.

Kliebenstein, D., Pedersen, D., Barker, B. and Mitchell-Olds, T. (2002a) Comparative analysis of quantitative trait loci controlling glucosinolates, myrosinase and insect resistance in *Arabidapsis thaliana*. *Genetics*, **161**, 325–332.

Kliebenstein, D.J., Figuth, A. and Mitchell-Olds, T. (2002b) Genetic architecture of plastic methyl jasmonate responses in *Arabidopsis thaliana*. *Genetics*, **161**, 1685–1696.

Levy, M., Wang, Q.M., Kaspi, R., Parrella, M.P. and Abel, S. (2005) Arabidopsis IQD1, a novel calmodulin-binding nuclear protein, stimulates glucosinolate accumulation and plant defense. *Plant J.* **43**, 79–96.

Manici, L.M., Lazzeri, L., Baruzzi, G., Leoni, O., Galletti, S. and Palmieri, S. (2000) Suppressive activity of some glucosinolate enzyme degradation products on Pythium irregulare and Rhizoctonia solani in sterile soil. *Pest Manag. Sci.* **56**, 921–926.

Mari, M., Iori, R., Leoni, O. and Marchi, A. (1996) Bioassays of glucosinolate-derived isothiocyanates against postharvest pear pathogens. *Plant Pathol.* **45**, 753–760.

Martin, N. and Müller, C. (2007) Induction of plant responses by a sequestering insect: relationship of glucosinolate concentration and myrosinase activity. *Basic Appl. Ecol.* **8**, 13–25.

Mewis, I., Appel, H.M., Hom, A., Raina, R. and Schultz, J.C. (2005) Major signaling pathways modulate Arabidopsis glucosinolate accumulation and response to both phloem-feeding and chewing insects. *Plant Physiol.* **138**, 1149–1162.

Mikkelsen, M.D., Hansen, C.H., Wittstock, U. and Halkier, B.A. (2000) Cytochrome P450 CYP79B2 from Arabidopsis catalyzes the conversion of tryptophan to indole-3-acetaldoxime, a precursor of indole glucosinolates and indole-3-acetic acid. *J. Biol. Chem.* **275**, 33712–33717.

Mikkelsen, M.D., Petersen, B.L., Glawischnig, E., Jensen, A.B., Andreasson, E. and Halkier, B.A. (2003) Modulation of CYP79 genes and glucosinolate profiles in Arabidopsis by defense signaling pathways. *Plant Physiol.* **131**, 298–308.

Mithen, R. (2001) Glucosinolates - biochemistry, genetics and biological activity. *Plant Growth Regul.* **34**, 91–103.

Mithen, R., Faulkner, K., Magrath, R., Rose, P., Williamson, G. and Marquez, J. (2003) Development of isothiocyanate-enriched broccoli, and its enhanced ability to induce phase 2 detoxification enzymes in mammalian cells. *Theor. Appl. Genetics*, **106**, 727–734.

Müller, A. and Weiler, E.W. (2000) Indolic constituents and indole-3-acetic acid biosynthesis in the wild-type and a tryptophan auxotroph mutant of *Arabidopsis thaliana*. *Planta*, **211**, 855–863.

Nair, R. and Rost, B. (2005) Mimicking cellular sorting improves prediction of subcellular localization. *J. Mol. Biol.* **348**, 85–100.

Naur, P., Petersen, B.L., Mikkelsen, M.D., Bak, S., Rasmussen, H., Olsen, C.E. and Halkier, B.A. (2003) CYP83A1 and CYP83B1, two nonredundant cytochrome P450 enzymes metabolizing oximes in the biosynthesis of glucosinolates in Arabidopsis. *Plant Physiol.* **133**, 63–72.

Neff, M.M., Nguyen, S.M., Malancharuvil, E.J. *et al.* (1999) BAS1: a gene regulating brassinosteroid levels and light responsiveness in Arabidopsis. *Proc. Natl. Acad. Sci. USA*, **96**, 15316–15223.

Petersen, B.L., Chen, S.X., Hansen, C.H., Olsen, C.E. and Halkier, B.A. (2002) Composition and content of glucosinolates in developing *Arabidopsis thaliana*. *Planta*, **214**, 562–571.

Piotrowski, M., Schemenewitz, A., Lopukhina, A., Müller, A., Janowitz, T., Weiler, E.W. and Oecking, C. (2004) Desulfoglucosinolate sulfotransferases from *Arabidopsis thaliana* catalyze the final step in the biosynthesis of the glucosinolate core structure. *J. Biol. Chem.* **279**, 50717–50725.

Pollmann, S., Müller, A., Piotrowski, M. and Weiler, E.W. (2002) Occurence and formation of indole-3-acetamide in *Arabidopsis thaliana*. *Planta*, **216**, 155–161.

Pollmann, S., Müller, A. and Weiler, E.W. (2006) Many roads lead to ''auxin'': of nitrilases, synthases, and amidases. *Plant Biol.* **8**, 326–333.

Rask, L., Andreasson, E., Ekbom, B., Eriksson, S., Pontoppidan, B. and Meijer, J. (2000) Myrosinase: gene family evolution and herbivore defense in Brassicaceae. *Plant Mol. Biol.* **42**, 93–113.

Reichelt, M., Brown, P.D., Schneider, B., Oldham, N.J., Stauber, E., Tokuhisa, J., Kliebenstein, D.J., Mitchell-Olds, T. and Gershenzon, J. (2002) Benzoic acid glucosinolate esters and other glucosinolates from *Arabidopsis thaliana*. *Phytochemistry*, **59**, 663–671.

Reintanz, B., Lehnen, M., Reichelt, M., Gershenzon, J., Kowalczyk, M., Sandberg, G., Godde, M., Uhl, R. and Palme, K. (2001) *bus*, a bushy Arabidopsis *CYP79F1* knockout mutant with abolished synthesis of short-chain aliphatic glucosinolates. *Plant Cell*, **13**, 351–367.

Rosso, M.G., Li, Y., Strizhov, N., Reiss, B., Dekker, K.A. and Weisshaar, B. (2003) An *Arabidopsis thaliana* T-DNA mutagenized population (GABI-Kat) for flanking sequence tag-based reverse genetics. *Plant Mol. Biol.* **53**, 247–259.

Schneider, A., Kirch, T., Gigolashvili, T., Mock, H.P., Sonnewald, U., Simon, R., Flügge, U.I. and Werr, W. (2005) A transposon-based activation-tagging population in *Arabidopsis thaliana* (TAMARA) and its application in the identification of dominant developmental and metabolic mutations. *FEBS Lett.* **579**, 4622–4628.

Shapiro, T.A., Fahey, J.W., Wade, K.L., Stephenson, K.K. and Talalay, P. (1998) Human metabolism and excretion of cancer chemoprotective glucosinolates and isothiocyanates of cruciferous vegetables. *Cancer Epidem. Biom. Prev.* **7**, 1091–1100.

Skirycz, A., Reichelt, M., Burow, M. *et al.* (2006) DOF transcription factor AtDof1.1 (OBP2) is part of a regulatory network controlling glucosinolate biosynthesis in Arabidopsis. *Plant J.* **47**, 10–24.

Smolen, G. and Bender, J. (2002) Arabidopsis cytochrome P450 cyp83B1 mutations activate the tryptophan biosynthetic pathway. *Genetics*, **160**, 323–332.

Stepanova, A.N., Hoyt, J.M., Hamilton, A.A. and Alonso, J.M. (2005) A link between ethylene and auxin uncovered by the characterization of two root-specific ethylene-insensitive mutants in Arabidopsis. *Plant Cell*, **17**, 2230–2242.

Stracke, R., Werber, M. and Weisshaar, B. (2001) The R2R3-MYB gene family in *Arabidopsis thaliana*. *Curr. Opin. Plant Biol.* **4**, 447–456.

Vancanneyt, G., Schmidt, R., Oconnorsanchez, A., Willmitzer, L. and Rochasosa, M. (1990) Construction of an intron-containing marker Gene - splicing of the intron in transgenic plants and its use in monitoring early events in Agrobacterium-mediated plant transformation. *Mol. Gen. Genetics*, **220**, 245–250.

Voinnet, O., Pinto, Y.M. and Baulcombe, D.C. (1999) Suppression of gene silencing: a general strategy used by diverse DNA and RNA viruses of plants. *Proc. Natl. Acad. Sci. USA*, **96**, 14147–14152.

Zhao, Y.D., Hull, A.K., Gupta, N.R., Goss, K.A., Alonso, J., Ecker, J.R., Normanly, J., Chory, J. and Celenza, J.L. (2002) Trp-dependent auxin biosynthesis in Arabidopsis: involvement of cytochrome P450s CYP79B2 and CYP79B3. *Genes Dev.* **16**, 3100–3112.

Zimmermann, P., Hirsch-Hoffmann, M., Hennig, L. and Gruissem, W. (2004) GENEVESTIGATOR. Arabidopsis microarray database and analysis toolbox. *Plant Physiol.* **136**, 2621–2632.

